

Fragmentation of cyclobutoxychlorocarbene: the cyclopropylcarbinyl/cyclobutyl cations revisited[†]

Robert A. Moss,* Fengmei Zheng, Lauren A. Johnson and Ronald R. Sauers

Department of Chemistry, Rutgers, The State University, New Brunswick, New Jersey 08903, USA

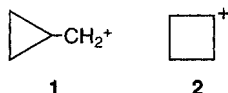
Received 21 November 2000; revised 13 January 2001; accepted 19 January 2001

ABSTRACT: Fragmentations of cyclobutoxychlorocarbene (**13**, $k_{\text{frag}} = 7.1 \times 10^5 \text{ s}^{-1}$) and cyclopropylmethoxychlorocarbene (**14**, $k_{\text{frag}} = 7.6 \times 10^5 \text{ s}^{-1}$) in MeCN proceed to tight and distinct $[\text{R}^+ \text{OC Cl}^-]$ ion pairs, which collapse to different distributions of cyclopropylcarbinyl, cyclobutyl and allylcarbinyl chlorides. B3LYP/6–31G* calculations support these conclusions, affording computed fragmentation activation energies of 6.4 (**13**) and 3.0 (**14**) kcal mol^{−1}. Copyright © 2001 John Wiley & Sons, Ltd.

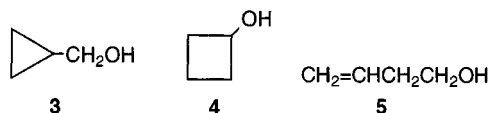
KEYWORDS: cyclobutoxychlorocarbene; fragmentation; cyclopropylcarbinyl cation; cyclobutyl cation

INTRODUCTION

The mechanistic interrelation of the cyclopropylcarbinyl (**1**) and cyclobutyl (**2**) cations is a classical triumph of early physical organic chemistry.¹ When either carbocation is in a 'free' state and a polar solvent (e.g. as generated from the alkyldiazonium cations produced by



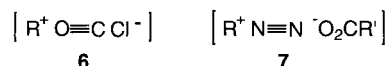
the aqueous nitrous acid deaminations of the corresponding amines), rapid 1,2-C shift rearrangements interconvert **1** and **2**, and 'scramble' labeled carbon atoms within each carbocation.¹ Nitrous acid deamination of either cyclopropylcarbinylamine or cyclobutylamine leads to cyclopropylmethanol (**3**), cyclobutanol (**4**) and 3-butenol (**5**);^{1b} a typical distribution is 52:44:4.^{1c,2}



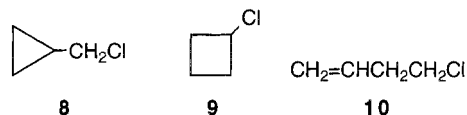
When, however, the cyclopropylmethyldiazonium cation is generated in a moderately polar solvent as part of an *ion pair* (e.g. $\text{RN}_2^+ \text{O}_2\text{CR}'^-$), rapid anion capture of the successor alkyl cation is facilitated, leading to a product mixture rich in the cyclopropylmethyl ester. For

example, reaction of cyclopropyldiazomethane with ethereal benzoic acid affords the benzoate esters of **3**, **4** and **5** in the distribution 79.2:13.6:7.2.² The cyclopropyl-to-cyclobutyl ratio, which is ~1.2 in the nitrous acid deamination reactions, increases to ~5.8 in the ion pair process.

We found that fragmentations of alkoxychlorocarbenes³ lead to ion pairs that resemble those of deaminative processes.⁴ Momentarily neglecting product 'memory effects' due to *cis* or *trans* ROCCl precursors³ (memory effects due to precursor geometry are known for nitrogen-separated ion pairs⁵), we can represent typical carbene-derived and diazonium-derived ion pairs as **6** and **7**, respectively. The similarity is apparent, even to the isoelectronic character of the CO and N₂ 'leaving groups.' When cyclopropylmethoxychlorocarbene fragments in MeCN at 23 °C, the distribution of cyclopropyl-



carbinyl chloride (**8**), cyclobutyl chloride (**9**) and 4-chloro-1-butene (**10**) is 78:15:7 (cyclopropylcarbinyl:



cyclobutyl = 5.2).⁶ This closely resembles the distribution of the esters formed from cyclopropyldiazomethane and benzoic acid in diethyl ether² (see above), suggesting that ion pairs **6** and **7** (R = cyclopropylcarbinyl) are good overall representations of the initial intermediates in these processes.

In our earlier work,⁶ however, we neither determined

*Correspondence to: R. A. Moss, Department of Chemistry, Rutgers, The State University, New Brunswick, New Jersey 08903, USA.

E-mail: moss@rutchem.rutgers.edu

[†]Dedicated to Professor Hans-Jörg Schneider in recognition of his 65th birthday.

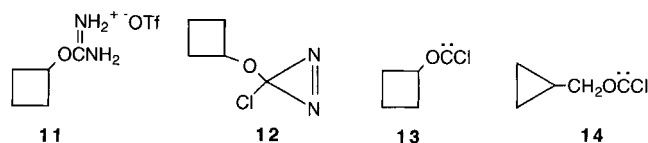
Contract/grant sponsor: National Science Foundation.

the rate constant for the fragmentation of cyclopropylmethoxychlorocarbene nor compared its kinetics and product distributions with analogous data for cyclobutoxychlorocarbene. Here, we provide these results, in addition to computational studies of these carbene fragmentations, enabling us to refine our mechanistic portrait of these reactions.

RESULTS AND DISCUSSION

Precursor and products

Cyclobutanol (**4**) was converted to the cyclobutyl isouronium triflate (**11**) by reaction with cyanamide and trifluoromethanesulfonic acid.⁷ Graham oxidation⁸ of **11** with hypochlorite then afforded 3-cyclobutoxy-3-chlorodiazirine (**12**), which was purified by chromatography

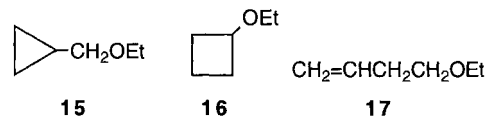


(silica gel/pentane). The pentane solvent was removed evaporatively and replaced with either MeCN or 1,2-dichloroethane (DCE) for kinetic and product studies. UV maxima were observed for **12** at 352 and 367 nm (pentane), 354 and 368 nm (MeCN) and 353 and 367 nm (DCE).

Photolysis ($\lambda > 320$ nm) of diazirine **12** ($A_{\lambda_{\max}} = 1.0$) in MeCN or DCE generated cyclobutoxychlorocarbene (**13**), which fragmented to yield chlorides **8–10**. These products were identified by gas chromatography–mass spectrometry (GC–MS) and GC comparisons with authentic materials,⁶ while product distributions were ascertained by capillary GC analysis. The same products were formed from diazirine generated cyclopropylmethoxychlorocarbene (**14**).⁶ Table 1 gives the product distributions from the fragmentations of carbenes **13** and **14**.

When **13** and **14** were generated by diazirine photolysis in ethanol, or ethanol–MeCN mixtures, ethers **15**⁶ and **16**⁶

(with traces of **17**) formed in addition to chlorides **8–10**. Product distributions for the fragmentations of **13** and **14** in 100% ethanol are also given in Table 1.



In Fig. 1, we depict the relative yields of chlorides **8–10** and ethers **15** and **16** as a function of the mole fraction of ethanol in MeCN for the fragmentation of **13**. The yield of cyclobutyl chloride (**9**) decreases smoothly, whereas that of the corresponding ether (**16**) increases, with increasing ethanol. Cyclopropylcarbinyl chloride (**8**) and the analogous ether (**15**) present a similar profile. Remarkably, the cyclopropylmethyl-to-cyclobutyl ratios, **8:9** and **15:16**, remain reasonably constant at 1.4–1.6 for RCl and 0.66–0.96 for ROEt over the range of ethanol mole fractions, suggesting that the origins of the chlorides and ethers lie in distinct ion pairs.

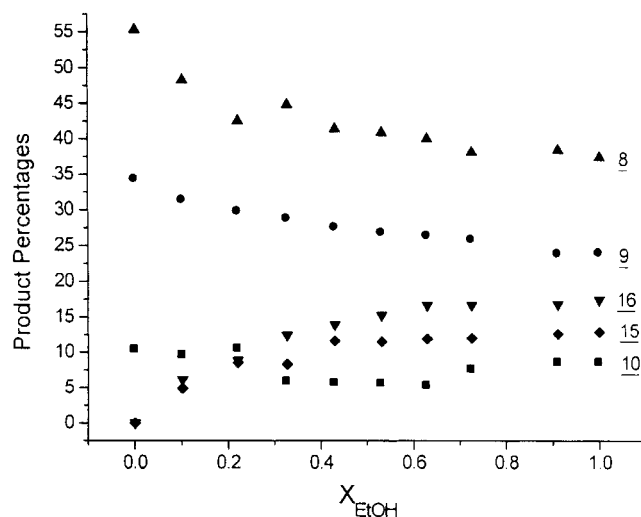


Figure 1. Product distributions (%) from the fragmentation of cyclobutoxychlorocarbene (**13**) in MeCN–EtOH as a function of the mole fraction (X) of ethanol. See text for product numbering

Table 1. Product distributions from fragmentations of carbenes **13** and **14**^a

Carbene	Solvent	Product distribution (%)						
		8	9	10	8:9^b	15	16	15:16^b
13	MeCN	55.3	34.3	10.3	1.6			
	DCE	64.5	29.8	5.6	2.2			
	EtOH	37.4	23.9	8.5	1.6	12.9	17.4	0.74
14	MeCN	73.3	17.1	9.6	4.3			
	MeCN ^c	78	15	7	5.2			
	EtOH	41.0	5.5	2.1	7.4	29.1	22.3	1.3

^a Diazirine precursors were photolyzed at 25 °C; product percentages refer to the total product.

^b Ratio of cyclopropylcarbinyl to cyclobutyl product.

^c Thermal generation of **14** at 25 °C; from Ref. 6.

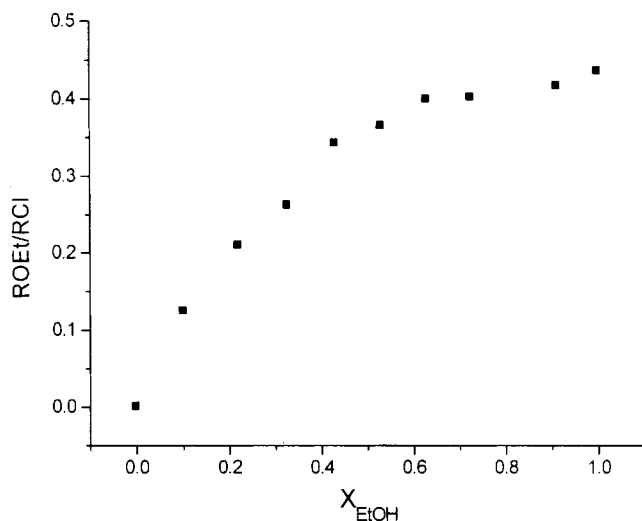
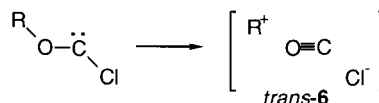
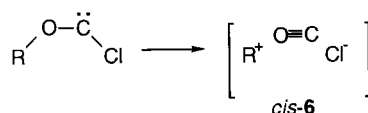


Figure 2. ROEt:RCl product ratio vs mole fraction of ethanol in acetonitrile for the fragmentation of cyclobutoxychlorocarbene (**13**)



Moreover, the ion pair(s) involved in the fragmentations of carbene **13** must be, at least in part, distinct from those arising from carbene **14**. In the latter case (Table 1), the **8:9** ratio of 4.3–7.4 is very much weighted toward cyclopropylmethyl chloride, whereas from carbene **13**, **8:9** is only 1.6–2.2, depending on solvent. Put another way, the **8:9** ratios ‘remember’ their origins: from the cyclopropylmethyl precursor (**14**), chloride mixtures rich in **8** result; from the cyclobutyl precursor (**13**), larger (although not dominant) yields of **9** are obtained.

Just as the **8:9** ratio in MeCN (4.3–5.2) from **14**, via **6**, resembles that obtained (5.6) from the ethereal cyclopropylmethyl diazonium benzoate ion pair (**7**),^{2,6} the **8:9** ratio found here for the fragmentation of carbene **13** (1.6 in MeCN) is similar to that observed (1.3) for the analogous ester products formed from cyclobutyldiazonium *p*-phenylazobenzoate ion pairs in 98% toluene–2% ethanol.⁹ The analogy between the ion pairs arising from carbene fragmentation and those from deaminative reactions is thereby strengthened.

We also note the persistence of RCl products in the fragmentations of either **13** or **14**, even in pure ethanol. Figure 2 traces the ROEt-to-RCl product ratios as a function of ethanol mole fraction in MeCN for fragmentations of carbene **13**. Analogous correlations have been published for the fragmentations of **14**⁶ and benzyloxychlorocarbene.^{6,10} At 100% ethanol, the RCl:ROEt ratios are 2.3 from **13** and 0.94 from **14** (Table 1). Ion pairs **6**, with chloride counterions, therefore persist in ethanol and, when R is initially cyclobutyl, account for about two-thirds of the product mixture. When R is initially

cyclopropylcarbonyl, ion pairs **6** give rise to slightly less than half of the products. In both instances, ethers **15** and **16** comprise the balance of the product mixtures.

The ether product ratios (**15:16**) in Table 1 reveal only small precursor memory effects and are much closer to 1.0 whether they stem from carbene **13** or **14**. These **15:16** distributions approach the cyclopropylcarbonyl-to-cyclobutyl ratios obtained from the ‘free’ cations formed in nitrous acid deamination reactions (1.1–1.3).^{1,2} Clearly, the ultimate ionic precursors of chlorides **8** and **9** differ from those of ethers **15** and **16**.

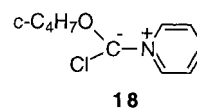
Interconversion of cations **1** and **2** within ion pairs **6** is in competition with ion pair collapse, solvolysis by ethanol and diversion to ion pairs in which [−]OEt replaces Cl[−]. The dynamics of these processes are complex and governed by only small enthalpy and entropy differences between the different species. An additional complication concerns the geometry of ion pair **6**, which may initially arise as *cis*-**6** or *trans*-**6**,^{3,6} depending on the geometry of

the precursor ROCCl [where rotation around the central O—C bond is opposed by ~15–18 kcal mol^{−1} (1 kcal = 4.184 kJ) due to partial double bond character].¹¹ We have speculated^{3,6} that *cis*-**6**, in which CO does not ‘insulate’ R⁺ from Cl[−], may be largely responsible for the RCl product formed by ion pair return in ethanol, whereas *trans*-**6**, in which CO is interposed between R⁺ and Cl[−], may be more readily intercepted by ethanol, mainly affording ROEt. No direct test of this idea is available.

KINETICS

Although rate constants for the decompositions of most alkyldiazonium cations are unknown because of their exceedingly facile fragmentation,¹² rate constants for the fragmentation of ROCCl can be measured by laser flash photolysis (LFP).^{3,13}

Absolute rate constants for the fragmentations of carbenes **13** and **14** were determined by LFP¹⁴ using the pyridine ylide methodology.¹⁵ For example, LFP at 351 nm and 25 °C of diazirine **12** in MeCN or DCE (A ≈ 1.0 at λ_{max}) in the presence of pyridine produced an absorbance at 412 nm due to ylide **18**. In MeCN,



correlation of the apparent rate constants for ylide

Table 2. Rate constants for carbene fragmentation^a

Carbene	k_{frag} (s ⁻¹) ^b	
	MeCN	DCE
13	7.1×10^5	3.2×10^5
14	7.6×10^5	8.6×10^4

^a At 25 °C.^b Errors, 10–15%.

formation, k_{obs} ($1.10\text{--}2.15 \times 10^6 \text{ s}^{-1}$), vs pyridine concentration ($1.65\text{--}7.42 \text{ M}$) was linear (seven points, $r = 0.994$) with a slope of $1.59 \times 10^5 \text{ l mol}^{-1} \text{ s}^{-1}$ and a y-intercept of $7.14 \times 10^5 \text{ s}^{-1}$. The former value is the second-order rate constant for ylide formation from carbene **13** and pyridine, whereas the latter value can be equated with k_{frag} for **13** → **6** (R = cyclobutyl) because the product studies show that only fragmentation products arise from cyclobutoxychlorocarbene.

Kinetic data for the fragmentations of **13** and **14** in both MeCN and DCE are given in Table 2. There is some indication of a solvent effect between DCE ($\epsilon = 10.7$) and the more polar MeCN ($\epsilon = 36.6$); k_{frag} is 2.2 (**13**) to 8.8 (**14**) times smaller in DCE than in MeCN.¹⁶ However, the important observation is the similarity of k_{frag} for **13** and **14**, which fragment in, e.g., MeCN at $7 \times 10^5\text{--}8 \times 10^5 \text{ s}^{-1}$.

In contrast, in acetolysis reactions, cyclopropylcarbinyl tosylate is considerably more reactive than cyclobutyl tosylate: the respective enthalpies of activation are 16.7 (Ref. 17) and 30 (Ref. 18) kcal mol⁻¹, with corresponding rate constants at 50 °C of $\sim 2.4 \times 10^{-3} \text{ s}^{-1}$ (extrapolated from the 25 °C data¹⁷) and $3.4 \times 10^{-5} \text{ s}^{-1}$,¹⁸ respectively. This rate differential arises mainly because the solvolysis of the cyclopropylcarbinyl tosylate is strongly assisted by formation of the 'bisected' cyclopropylmethyl cation, where electron donation from the strained ring's proximal p-rich σ -bonds efficiently stabilizes the developing carbocation.^{1a}

Fragmentations of carbenes **13** and **14**, however, proceed through early transition states and over low activation barriers, where there is relatively little call for the potential electronic stabilization available in the cyclopropyl ring of **14**. Attempts to measure E_a for the fragmentation of **13** in MeCN (–20 to 30 °C) gave k_{frag} values that showed little temperature dependence, and scattered about a nearly horizontal ($E_a \approx 0$) correlation line. Scatter was also observed for k_{frag} of **14** below 15 °C. In our experience, these abortive Arrhenius correlations imply low activation energies ($E_a < 3\text{--}4 \text{ kcal mol}^{-1}$). Indeed, computed E_a s for the fragmentations of **13** and **14** are 6.4 and 3.0 kcal mol⁻¹, respectively, in MeCN (see below).

Although the low activation energies and concomitant early transition states for the fragmentations of **13** and **14** suppress differences in k_{frag} , we note that the cyclobu-

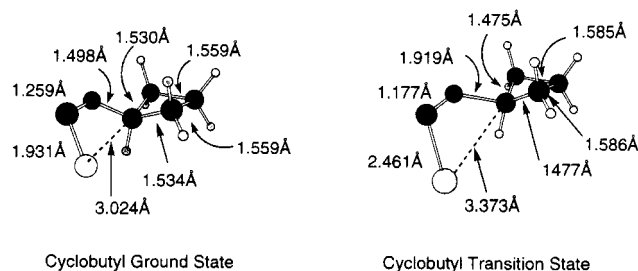


Figure 3. B3LYP/6–31G* ground state and fragmentation transition state for *cis*-cyclobutoxychlorocarbene (*cis*-**13**) in SCI-PCM simulated MeCN. See text for computational details

toxychlorocarbene fragmentation rate constant is about twice that for benzyloxychlorocarbene ($\sim 4 \times 10^5 \text{ s}^{-1}$),^{13,16} and ~ 10 times greater than k_{frag} for cyclopentoxychlorocarbene ($\sim 8 \times 10^4 \text{ s}^{-1}$) (L. A. Johnson and R. A. Moss, unpublished work). Small residual electronic stabilizations may therefore operate even in the 'early' fragmentation transition states of **13** and **14**.

COMPUTATIONAL STUDIES

In analogy with our previous computational studies of alkoxyhalocarbene fragmentation,^{11a} we computed ground-state and fragmentation transition states (TS) for (*cis*) carbenes **13** and **14**. All structures were fully optimized by analytical gradient methods at the B3LYP/6–31G* level using the Gaussian94 suite of programs (the optimization used Gaussian94 Revision B.1 and default convergence criteria¹⁹ and DFT calculations used Becke's three-parameter hybrid method using the LYP correlation functional²⁰). Computed (unscaled) gas-phase energies were corrected for thermal effects at 298.15 K and for zero-point energy differences. Normal coordinate analyses confirmed the nature of the ground- and transition-state structures. To simulate the MeCN solvent ($\epsilon = 36.64$) in which the fragmentations were studied, we employed the SCI-PCM computational model, with full geometry optimization.

The computed ground and transition states for carbenes **13** and **14** (both in MeCN) appear in Figs 3 and 4, respectively. In each TS, the C–Cl and (alkyl) C–O bonds are in the process of breaking: C–Cl distances increase from 1.93 to 2.46 Å (**13**) and from 1.94 to 2.33 Å (**14**), while parallel increases occur for C–O distances: from 1.50 to 1.92 Å (**13**) and from 1.52 to 1.85 Å (**14**). Simultaneously, the (carbene) C–O bonds of **13** and **14** contract from 1.25–1.26 to 1.18–1.19 Å, en route to the C≡O bond length of 1.128 Å.

Another point deserves mention: the close proximities of the nascent chloride anions and C(δ^+) in the transition states (3.37 Å for **13** and 3.36 Å for **14**) point toward the subsequent formation of (*cis*) ion pairs **6**. Indeed, intrinsic

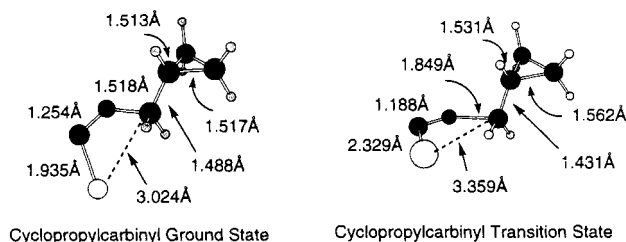


Figure 4. B3LYP/6-31G* ground state and fragmentation transition state for *cis*-cyclopropylmethoxychlorocarbene (*cis*-**14**) in SCI-PCM simulated MeCN. See text for computational details

reactivity coordinate (irc) calculations were carried out starting from the transition states of Figs 3 and 4. With the cyclopropylcarbonyl system in MeCN (Fig. 4), the energy and structure evolved in two directions: backward toward ground-state carbene **14**, and forward toward the ion pair shown in Fig. 5(left), which displays the geometry associated with the 'bisected' form of the cyclopropylcarbonyl cation.^{1a} Note that the C—Cl separation in this ion pair is 3.48 Å, not very different from the 3.36 Å separation in the corresponding transition state (Fig. 4). In contrast, the C—O and C(carbene)—Cl separations of the ion pair (2.60 and 2.94 Å, respectively) greatly increase, relative to the analogous separations in the fragmentation transition state (1.85 Å and 2.33 Å, respectively). Interestingly, the energy of the ion pair—CO assemblage is computed to be ~ 4.4 kcal mol⁻¹ lower than that of carbene **14**. Thus, in MeCN, we calculate that cyclopropylmethoxychlorocarbene exothermically fragments to an ion pair, with the latter separated from the carbene by a barrier of only 3.0 kcal mol⁻¹.

An irc treatment of the transition state for the fragmentation of **13** (Fig. 3) proceeded only to the ground-state geometry when the calculation was carried out in simulated MeCN. In vacuum, the irc led backward to the ground state and forward to the ion pair—CO assemblage shown in Fig. 5(right), where the carbon framework corresponds to that computed for the bicyclobutonium ion. The geometries computed for the ion pairs in Fig. 5 closely correspond to those computed

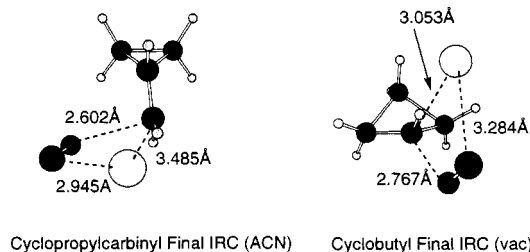


Figure 5. Product endpoints of irc computations carried out starting from the respective transition states: left, carbene **14** (in MeCN); right, carbene **13** (gas phase)

by Koch *et al.*^{21a} Small differences can be attributed to the presence of the counterion and carbon monoxide.^{21b} As in the fragmentation of **14**, so too with **13**, the cyclobutyl C—O and C(carbene)—Cl separations continually increase (*in vacuo*) from ground state to transition state to ion pair (for **13** the interatomic distances are given for *gas-phase* ground state, transition state and ion pair), from 1.48 to 2.16 to 2.77 Å for C—O and 1.89 to 2.64 to 3.28 for C—Cl. The CO molecule is clearly departing. The behavior of the cyclobutyl C—Cl separation, however, is different, *contracting* from 3.10 Å in the transition state^{21b} to 3.05 Å in the ion pair (Fig. 5). This contraction must, in part, reflect the absence of polar solvent in the calculation, making the C(δ^+)—Cl(δ^-) interaction even more important than it is in the cyclopropylcarbonyl system (see above), where MeCN is simulated, and stabilizes the ion pair {in the gas phase, the 'bicyclobutonium' chloride ion pair is 5.7 kcal mol⁻¹ higher in energy than the carbene (**13**) from which it derives. No doubt, in MeCN, the ion pair would be significantly lower in energy. Note that the activation energy for the fragmentation of **13** is computed to be much lower in MeCN (6.4 kcal mol⁻¹) than *in vacuo* (20.3 kcal mol⁻¹), largely due to preferential stabilization of the polar transition state (Fig. 3) by MeCN. [The parallel computed reduction in E_a induced by solvation in the fragmentation of **14** is 17.8 (vacuum) vs 3.0 kcal mol⁻¹ (MeCN)]. In this latter case, the C(δ^+)—Cl(δ^-) distance increases slightly (from 3.36 to 3.48 Å) on going from the transition state to the ion pair (see above).

Clearly, the alkyl groups of carbenes **13** and **14** retain distinctive characters in their fragmentation transition states (Figs 3 and 4), and in the ion pairs that result from the fragmentations (Fig. 5).

Activation energies were obtained for the fragmentations of **13** and **14** in MeCN as differences between the computed transition-state and ground-state energies; we obtained $E_a = 6.4$ (**13**) and 3.0 (**14**) kcal mol⁻¹. A small residue of the substantial acetolysis $\Delta\Delta H^\ddagger$ between cyclopropylcarbonyl and cyclobutyl tosylates (~ 13 kcal mol⁻¹, see above) is apparent in the computed E_a s; $\Delta E_a \approx 3.4$ kcal mol⁻¹ in favor of **14**. However, the computed E_a s are fairly low, consistent with the observed rapid fragmentation rates of the carbenes (Table 2), and with the 'early' transition states depicted in Figs 3 and 4. The E_a s computed for the fragmentations of **13** and **14** in MeCN are bracketed by those calculated for the other (*cis*) ROCCl in MeOH,¹¹ including Me₂CHOCCl (8.0 kcal mol⁻¹) and PhCH₂OCCl (1.4 kcal mol⁻¹).

CONCLUSIONS

Fragmentations of cyclobutoxychlorocarbene (**13**) and cyclopropylmethoxychlorocarbene (**14**) in MeCN generate distinct ion pairs consisting of an alkyl cation,

carbon monoxide and a chloride anion. Although subsequent, reversible interconverting rearrangements of the alkyl cations occur competitively with ion pair collapse, the latter process dominates, so that distinct product distributions of chlorides **8–10** are formed from each carbene. Differences in product distributions persist, although to a smaller extent, in the formation of ethers **15** and **16** from the fragmentations of carbenes **13** or **14** in ethanol. Computational studies support the generation of distinct ion pairs from each carbene, and further suggest that the cationic components of the ion pairs derived from **13** or **14** resemble the bicyclobutonium cation or the bisected cyclopropylmethyl cation, respectively.^{21a} The rate constants for the fragmentations of carbenes **13** and **14** in MeCN were determined by LFP as 7.1×10^5 and $7.6 \times 10^5 \text{ s}^{-1}$, respectively. The similarity in rate constants reflects the low activation energies of the fragmentations, which are calculated (B3LYP/6–31G*) as 6.4 (**13**) and 3.0 (**14**) kcal mol⁻¹ in MeCN.

EXPERIMENTAL

Solvents. Acetonitrile and pyridine (both Fisher, Certified, ACS) were dried by refluxing over CaH₂, followed by distillation, and storage over 5A molecular sieves. Dichloroethane (Aldrich, Certified, ACS) was used as received. Pentane (Fisher, HPLC grade) was stored over 5A molecular sieves.

Cyclobutanol²². Cyclopropylcarbinol (10 g, 0.14 mol) and 50 ml of 2.0 M aqueous HCl solution were heated at 85 °C for 2 h until a clear solution was obtained. This solution was extracted with 3 × 20 ml of diethyl ether, and the combined extract was dried over MgSO₄. Filtration and rotary evaporation afforded 15 ml of liquid that was distilled through a microscale spinning band column. The fraction with bp 121–124 °C was collected as cyclobutanol.

¹H NMR (200 MHz) (δ , DMSO-*d*₆): 4.02 (m, 1H, CHOH), 2.10 (m, 2H), 1.80 (m, 2H), 1.20–1.60 (m, 2H) [the NMR spectrum (No. 1763) appears in the Sadtler collection;²³ the b.p. is also given there as 123 °C/733 mmHg].

Cyclobutylisouronium trifluoromethanesulfonate (11). This compound was prepared by the method in Ref. 7. In a 50 ml round-bottomed flask, equipped with a stirring bar and protected with a CaCl₂ tube, were placed 0.73 g (17.4 mmol) of cyanamide, 5.0 g (69.4 mmol) of cyclobutanol and 10 ml of dry THF. To this solution was added 1.67 g (17.4 mmol) of trifluoromethanesulfonic acid. The mixture was stirred magnetically at 25 °C for 30 h, then diluted with 200 ml of dry diethyl ether, sealed and placed in the refrigerator. A light-brown oil formed, which was separated and stored at 25 °C for 1 week, whereupon white crystals appeared. The crystals were

harvested, washed with diethyl ether and dried *in vacuo* to afford 54% of the title salt, m.p. 69–70 °C.

¹H NMR (δ , DMSO-*d*₆): 8.30 (br, s, 4H NH₂), 4.93 (m, 1H, CHO), 2.46, 2.07, 1.80, 1.54 (ms, 6H, cyclobutyl). Anal. Calculated for C₆H₁₁F₃N₂O₄S: C, 27.26; H, 4.20; N, 10.61. Found: C, 27.25; H, 4.26; N, 10.63%.

3-Cyclobutoxy-3-chlorodiazirine (12). The general method of Graham⁸ was followed. To 3.5 g of LiCl in 100 ml of DMSO were added 1.0 g (3.8 mmol) of isouronium salt **11** and 50 ml of pentane. The mixture was cooled to 20 °C and stirred magnetically. Then, 200 ml of 12% commercial aqueous sodium hypochlorite solution ('pool chlorine'), saturated with NaCl, were slowly added. Stirring was continued for 15 min at 15 °C after the addition had been completed. The reaction mixture was poured into 150 ml of ice–water in a large separating funnel. The aqueous phase was removed and the pentane layer was washed twice with 75 ml portions of ice–water and then dried for 2 h over CaCl₂ at 0 °C. The diazirine–pentane solution was purified by chromatography over silica gel with pentane as eluent. Pentane was removed by rotary evaporation and replaced by MeCN or DCE to a volume of ~30 ml. The UV maxima of **12** in pentane, MeCN, and DCE are described in the text.

¹H NMR (δ , CD₃CN): 4.2–4.4 (m, 1H, CHO), 1.9–2.0, 1.5–1.8, 1.2–1.5 (ms, 6H, cyclobutyl). Details of the preparation of cyclopropylmethylisouronium tosylate and of cyclopropylmethoxychlorodiazirine can be found in Refs 6 and 24. Authentic samples of chloride products **8–10** and ether products **15** and **16**, are also described in these sources, and in references cited there in.

Diazirine photolysis. Solutions of diazirine **12** in MeCN, DCE or MeCN–EtOH (*A* = 1.0 at λ_{max}) were photolyzed at 25 °C for 1 h with a focused Oriel UV lamp, $\lambda > 320 \text{ nm}$ (uranium glass filter). The products were analyzed by capillary GC and GC–MS, using a 30 m × 0.25 mm i.d., 0.25 μm film thickness CP–Sil 5CB (100% dimethylpolysiloxane) column at 25 °C (4 min, programmed to 80 °C at 10 °C min⁻¹). Products, which were confirmed by GC and GC–MS comparisons to authentic samples,⁶ are described above (cf. Table 1).

Laser flash photolytic studies employed our LFP system, which is described in detail elsewhere.¹⁴

Acknowledgments

We are grateful to the National Science Foundation for financial support. Access to the computational resources of the Center for Computational Neuroscience at Rutgers University (Newark) is much appreciated.

REFERENCES

1. (a) Lowry TH, Richardson KS. *Mechanism and Theory in Organic Chemistry* (3rd edn). Harper and Row: New York, 1987; 454–463; (b) Mazur RH, White WN, Seminow DA, Lee CC, Silver MS, Roberts JD. *J. Am. Chem. Soc.* 1959; **81**: 4390; (c) Renk E, Roberts JD. *J. Am. Chem. Soc.* 1961; **83**: 878; (d) Richey HG Jr. In *Carbonium Ions*, vol. III, Olah GA, Schleyer PvR (eds). Wiley–Interscience: New York, 1972, 1201ff; (e) Wiberg KB, Hess BA Jr, Ashe AJ III. In *Carbonium Ions*, vol. III, Olah GA, Schleyer PvR (eds). Wiley–Interscience: New York, 1972, 1295ff.
2. Moss RA, Shulman FC. *Tetrahedron* 1968; **24**: 2881.
3. Moss RA. *Acc. Chem. Res.* 1999; **32**: 969.
4. Moss RA. *Acc. Chem. Res.* 1974; **7**: 421.
5. Moss RA, Powell CE. *J. Am. Chem. Soc.* 1976; **98**: 283.
6. Moss RA, Ho GJ, Wilk BK. *Tetrahedron Lett.* 1989; **30**: 2473.
7. Moss RA, Kaczmarczyk GM, Johnson LA. *Synth. Commun.* 2000; **30**: 3233.
8. Graham WH. *J. Am. Chem. Soc.* 1965; **87**: 4396.
9. Applequist DE, McGreer DE. *J. Am. Chem. Soc.* 1960; **82**: 1965.
10. Moss RA, Wilk BK, Hadel LM. *Tetrahedron Lett.* 1987; **28**: 1969.
11. (a) Yan S, Sauers RR, Moss RA. *Org. Lett.* 1999; **1**: 1603; (b) Kesselmayr MA, Sheridan RS. *J. Am. Chem. Soc.* 1986; **108**: 99–107, 844–845.
12. Zollinger H. *Diazo Chemistry II*. VCH: Weinheim, 1995; 241–304.
13. Moss RA, Ge C-S, Maksimovic L. *J. Am. Chem. Soc.* 1996; **118**: 9792.
14. Moss RA, Johnson LA, Merrer DC, Lee GE Jr. *J. Am. Chem. Soc.* 1999; **121**: 5940.
15. Jackson JE, Soundararajan N, Platz MS, Liu MTH. *J. Am. Chem. Soc.* 1988; **110**: 5595.
16. Moss RA, Johnson LA, Yan S, Toscano JP, Showalter BM. *J. Am. Chem. Soc.* 2000; **122**: 11256.
17. Roberts DD. *J. Org. Chem.* 1964; **29**: 294.
18. Roberts JD, Chambers VC. *J. Am. Chem. Soc.* 1951; **73**: 5034.
19. Frisch MJ, Trucks GW, Schlegel HB, Gill PMW, Johnson BG, Robb MA, Cheeseman JR, Keith T, Petersson GA, Montgomery JA, Raghavachari K, Al-Laham MA, Zakrzewski VG, Ortiz JV, Foresman JB, Cioslowski J, Stefanov BB, Nanayakkara A, Challacombe M, Peng CY, Ayala PY, Chen W, Wong MW, Andres JL, Replogle ES, Gomperts R, Martin RL, Fox DJ, Binkley JS, Defrees DJ, Baker J, Stewart JP, Head-Gordon M, Gonzalez C, Pople JA. Gaussian94 Revision B. 1. Gaussian: Pittsburgh, PA, 1995.
20. Becke AD. *J. Chem. Phys.* 1993; **98**: 5648.
21. (a) Koch W, Liu B, DeFrees DJ. *J. Am. Chem. Soc.* 1988; **110**: 7325; (b) Saunders M, Laidig KE, Wiberg KB, Schleyer PvR. *J. Am. Chem. Soc.* 1988; **110**: 7652.
22. Lee CC, Cessna AJ. *Can. J. Chem.* 1980; **58**: 1075.
23. Simons WW (ed). *The Sadtler Handbook of Proton NMR Spectra*, vol. 2. Sadtler Research Laboratories: Philadelphia, PA, 1978; 760.
24. Ho G-J. PhD Dissertation, Rutgers University, New Brunswick, NJ, 1992.